SMALL OVERTOPPING AT ALBUFEIRA HARBOUR: FIELD MEASUREMENTS AND MODELLING

Ó. Ferreira[1], M.T. Reis[2], A.R. Carrasco[1], M.G. Neves[2], D. Neves[2] and E. Didier[2]

Abstract

Overtopping evaluation is often performed by empirical methods that still require complementary validation against field measurements. This study presents the first data set of overtopping measured at a breakwater in Portugal, including flow depths, velocities and discharges. Data were collected for small overtopping conditions (lower than $1.24*10^{-3}$ $m^3/s/m$) and compared with estimated values from empirical methods. The corrected NN_OVERTOPPING2 (corrected) tool proved to give reasonable estimations when the overall analyzed period was considered, while the uncorrected NN_OVERTOPPING2 and the EurOtop formulas were unable to adequately represent the measured discharges. Pn (normalized wave power) is suggested as a proxy to achieve discharge predictions using offshore wave parameters and the sea level (tide and surge).

1. Introduction

Wave overtopping is of principal concern for structures constructed primarily to defend against flood (Pullen *et al*., 2007). Overtopping studies have, therefore, paramount importance for the design of new coastal structures, risk assessment and warning systems. Overtopping discharge is often used to design sea dikes and breakwaters, while dike resilience should be evaluated by using flow velocities and overtopping flow depths (Norgaard *et al*., 2013). Overtopping evaluation (discharges, flow velocity and/or flow depth) has been determined by empirical formulations, neural network analysis, and both numerical and physical modelling. The EurOtop Manual (Pullen *et al*., 2007) gives guidance on many of such tools. Some of them may be difficult to use with input parameters being open to interpretation (McCabe *et al*., 2013). The existing formulas and performed validations are based on data from numerous physical models including a large number of small scale tests. Comparison between formulas output and field measurements is still scarce and the vast majority of the available data came from the European project CLASH (for details see www.clash.ugent.be) which collected the most important field data set on wave overtopping, allowing formulas calibration/validation and scale effects evaluation (De Rouck *et al*., 2005). Nonetheless, small overtopping discharges had never been subject of specific analysis. The present work analyses data from the first field campaign carried out in Portugal dedicated to measure wave overtopping discharges. The experiment was performed during "small overtopping conditions", near the hydrodynamic threshold for overtopping occurrence. The main purposes of this work are: (1) to characterise the overtopping at such limit conditions; (2) to define the relative importance of tidal level and wave power on local overtopping occurrence; and (3) to test the predictive reliability of commonly used empirical methods for these extreme conditions. For this last purpose, measured discharges were compared with empirical estimations based on the EurOtop formulae (Pullen *et al*., 2007) and the NN_OVERTOPPING2 tool (Coeveld *et al*., 2005).

2. Methods

Overtopping experiments were conducted at the west breakwater of Albufeira Harbour (South Portugal) on the 25th October 2012 (Figure 1) from 7 am till 4 pm (nearly one tidal cycle). The

[1] CIMA/UALG – Marine and Environmental Research Centre/University of Algarve, Campus de Gambelas, Building 7, 8005-139, Faro, Portugal. oferreir@ualg.pt, azarcos@ualg.pt

[2] LNEC – National Laboratory for Civil Engineering, Av. do Brasil, 101, 1700-066 Lisbon, Portugal. treis@lnec.pt, gneves@lnec.pt, dneves@lnec.pt, edidier@lnec.pt

chosen breakwater is of easy access, while it is often overtopped by waves higher than 3 m during spring tides. The collected and analysed data included tidal levels, wave characteristics (offshore and at the structure), and the obtained overtopping parameters (flow depth, velocity and associated discharge). The equipments were programmed, synchronized and deployed at the seaward slope and crest of the breakwater. All sensors were georeferenced using a DGPS.

Tidal data were obtained from Huelva (Spain) tide gauge, located at about 100 km to the East of the study area. The recorded levels (referred to the local harbour level) were corrected for the Portuguese datum and mean sea level (MSL). A time correction (~30 minutes tide delay in Albufeira) was also performed. Offshore wave height (significant, Hso, and maximum, Hmaxo) and peak period (Tp) were obtained from Faro's wave buoy (belonging to *Instituto Hidrográfico*), located 30 km to the East of the study area (Figure 1) at a depth contour of - 93 m MSL. The observation period (7 am to 4 pm) was split and analysed in blocks of 30 minutes. Hso and Tp were averaged for each block, while for Hmaxo the absolute maximum wave height within the 30 minutes was selected. To correctly compare offshore wave data with measurements performed at the breakwater, the travelling time of the waves from Albufeira to Faro buoy (in average 35 minutes for the measured period and dominant WSW direction) was subtracted. Offshore wave conditions were propagated to the breakwater toe (3.5 m below MSL) for further use at the empirical tools. The Wave Calculator (www.coastal.udel.edu/faculty/rad/), using linear wave theory, was employed for wave propagation, considering an offshore wave angle of 57º and the recorded Hso and Tp at Faro buoy. The Wave Calculator computed Hst, the significant wave height at the structure toe, for each 30 minutes block, and the wave angle with the structure, β, for the same location.

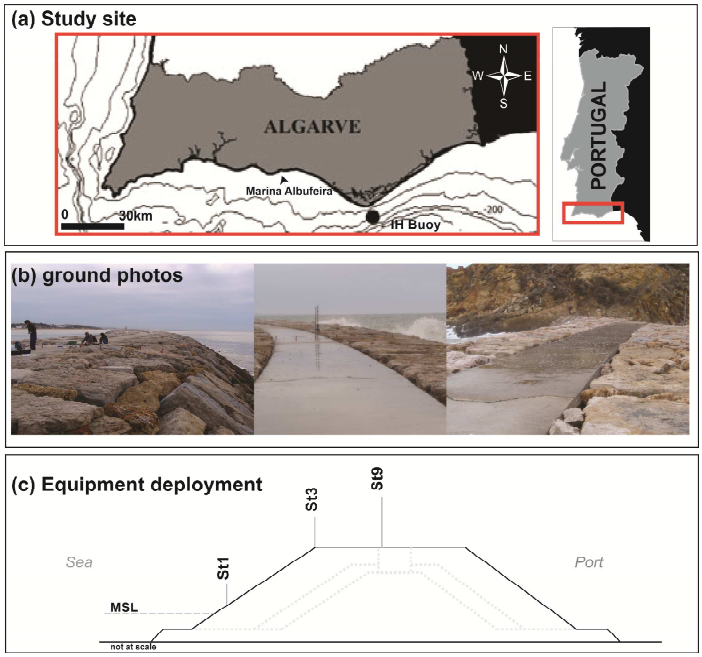

Figure 1. (a) Study area location; (b) Ground photographs of the breakwater crest including the measurement profile; and (c) distribution of the main pressure transducers along the measurement profile stations (St).

A normalised significant wave power (Pn) was computed, using a similar approach to Morris *et al.* (2001):

$$Pn = P\,(\frac{t30}{th}) \quad (1)$$

where P is the offshore wave power (using linear theory for computation), t30 is the tidal level at each 30 minutes block and th is the maximum tidal level during the experiment. At high tide

Pn = P, while at low tide Pn ~ 0.5P. Pn can be used as a proxy to define the enhanced overtopping potential during high tide and to reduce it at low tide, for similar wave conditions.

Data collected at stations St3 and St9 (Figure 1) were used to identify overtopping occurrence, and to determine flow depths and velocities. A flow depth baseline was defined by using a moving window (~20 records) and runup peaks were determined by extracting the change in flow depth relatively to the defined baseline. Only peaks higher than 2 times the PT error (mentioned by manufacturers) were used for discharge computations (conservative approach). For St3 (2 Hz acquisition rate; sensor placed 3.6 cm above the ground; manufacturer error of 0.5 cm), overtopping was only counted when the flow was higher than 1 cm above the sensor. Values below this threshold were considered within the sensor error although some of them might represent effective overtopping. For St9 (4 Hz acquisition rate; sensor placed 2.7 cm above the bed; manufacturer error of 0.3 cm) overtopping events were considered for records at least 0.6 cm above the sensor. Since sensors at St3 and St9 were placed 3.6 cm and 2.7 cm above the bed only overtopping with flow depths higher than 4.6 cm (St3) and 3.3 cm (St9) were used for analysis. Overtopping was analysed for each block of 30 minutes. The number of overtopping events (No), the average (Dav, in m) and the maximum (Dmax, in m) flow depth were determined, per block. Flow velocities were calculated for the six overtopping events crossing both St3 and St9 locations. The overtopping flow velocity (Uo, m/s) was defined as:

$$Uo = \frac{d(x9-x3)}{d(t9-t3)} \tag{2}$$

where d(x9-x3) is the horizontal distance between St9 and St3 (5.2 m) and d(t9-t3) is the difference in time (s) at which the flow peak passed St9 and St3 positions (Figure 2). An average flow velocity ($\bar{U}o$) was considered for discharge computation. Mean overtopping discharges per meter length of breakwater (Q, $m^3/s/m$) were then computed as:

$$Q = \frac{\bar{U}o \times Dav \times t}{1800} \tag{3}$$

where t is the integrated time of overtopping occurrence in each block and 1800 s corresponds to the total number of seconds in half-hour. Qst3 and Qst9 correspond to the discharges measured at St3 and St9 positions, respectively.

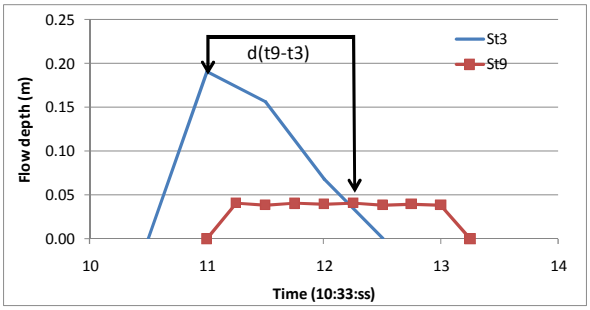

Figure 2. Overtopping flow depths at St3 (peaked flow) and St9 (laminar flow) and the used time interval to compute Q.

Video images from crest overtopping at the measurement profile (Figure 1) were recorded from a higher position at a nearby cliff (100 m in horizontal distance), for about 1 hour, near the maximum tidal level. Ground Control Points (GCPs) were placed and georeferenced to support overtopping flow analysis using video imagery.

Measured discharges were compared with mean overtopping discharges estimated by the EurOtop empirical formulas available online (http://www.overtopping-manual.com/calculation_tool.html) and the NN_OVERTOPPING2 tool (Coeveld *et al*., 2005). The geometrical characteristics of the structure adopted for calculations were defined according to six cross-sections measured around the instrumented profile (Figure 3).

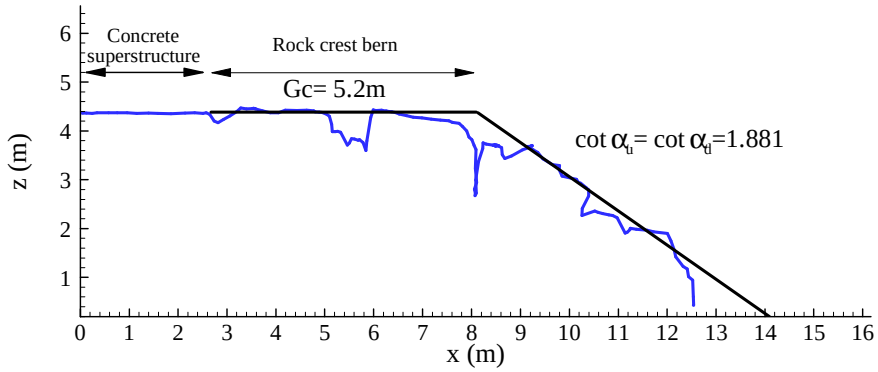

Figure 3. Cross-section near the instrumented profile and geometry adopted for overtopping calculations.

For the EurOtop formulas the structure geometry was assumed as "armoured composite slope with crest berm" (http://www.overtopping-manual.com/calculation_tool.html). The input wave parameters at the toe of the structure are the mean wave period (Tm-1,0) and the significant wave height (Hmo), both obtained from spectral analysis. Input structure parameters are the crest freeboard, Rc, the width of the structure crest, Gc, the front slopes, *cot* α_d and *cot* α_u, and the roughness/permeability coefficient for the armour material employed, γ (Figure 3). Tm-1,0 was calculated using the Tp value, assuming Tm-1,0=Tp/1.1. Hmo was considered as being equal to Hst and γ was assumed to be 0.5, in agreement with the value suggested in the EurOtop manual (Pullen *et al.*, 2007) for the block arrangement at the prototype structure. The results of mean overtopping discharges, Q, are presented per meter run of seawall.

Input wave parameters for the NN_ OVERTOPPING2 tool included the wave data at the toe of the structure (Tm-1,0 and Hst) and the angle between the wave direction and the normal to the structure, β, approximated here as a constant (~22º) after wave propagation. The twelve input geometrical parameters were derived from the breakwater geometry (Figure 3) and from the measured tidal level. These were: Rc, Gc, *cot* α_d, *cot* α_u and γ, used for the EurOtop formulas, and: the water depth in front of the structure, h; the water depth at the toe of the structure, ht; the width of the structure toe, Bt; the horizontal width of the structure berm, B; the water depth at the structure berm, hb; the slope of the structure berm, tan α_B; and the armour crest freeboard, Ac. The tool output consisted of the mean overtopping discharge, Q_NN; quantiles of several orders, Q_NN(2.5%), Q_NN(5%), Q_NN(25%), Q_NN(50%), Q_NN(75.5%), QNN_(95%) and Q_NN(97.5%), where the 95% confidence interval is defined using Q_NN(2.5%) and Q_NN(97.5%), that is [Q_NN(2.5%); Q_NN(97.5%)]; warnings and remarks related to the reliability of the predictions; and the corrected mean overtopping discharge, Q'_NN, that accounts for model effects, scale effects and wind effects in prototype situations.

3. Results

3.1 Waves and Tides

Tidal level ranged between -0.44 m and 1.18 m MSL (1.56 and 3.18 m above the Portuguese hydrographic datum, ZH; Figure 4) including a maximum storm surge of 0.18 m. Hso varied between 1.78 m and 2.41 m, while Hmaxo ranged between 3.07 m and 4.40 m, with the highest values occurring during ebb (Figure 4). Significant wave heights at the structure toe were smaller (1.55 m < Hst3 < 2.20 m) due to strong refraction (57º wave angle offshore to 22º at the structure toe). Tp had small variability through the monitored period with an average value of about 9 s.

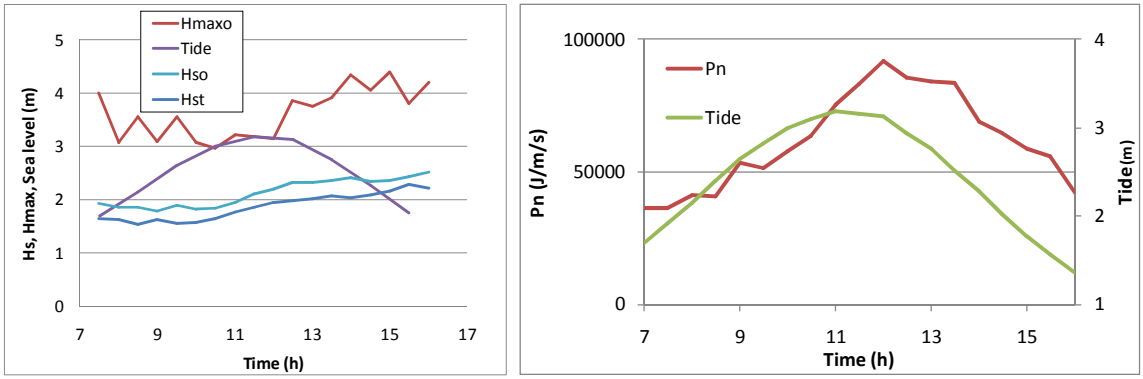

Figure 4. Tidal behaviour (referred to ZH), offshore (Hso, Hmaxo) and at the structure toe (Hst) wave heights (left panel), normalized wave power and tidal behaviour (right panel) along the studied period.

The normalized wave power (Pn) denotes an asymmetrical behaviour when compared with the tidal cycle (Figure 4, right panel). The asymmetry is induced by the increase on wave heights during ebb, which counteracted the effect of decreasing tidal level. The highest Pn values occurred immediately after high tide and at the beginning of ebb (from 12 am to 2 pm).

3.2 Measured Overtopping

A total of 41 overtopping events were recorded at St3 position (Figure 5). The distribution of overtopping events by 30 minutes blocks ranged from 0 (no measured events) at the beginning of the measurement period to 4-5 events immediately after high tide and during ebb. The average and maximum overtopping flow depths had a similar distribution and in general agreed with the number of events distribution (Figure 5). Dav ranged from 0 (no events) to circa 0.14 m, while Dmax reached 0.28 m at St3. Figure 5 (right panel) illustrates two of the observed overtopping events at St3. At Event 1 the peak first reaches the sensor – dominant situation for the majority of the observed flows - while at Event 2 the flow depth peak is centred at a middle position of the overtopping flow. Both events lasted 2 s, while in several cases the computed duration was $\leq$ 1.5 s.

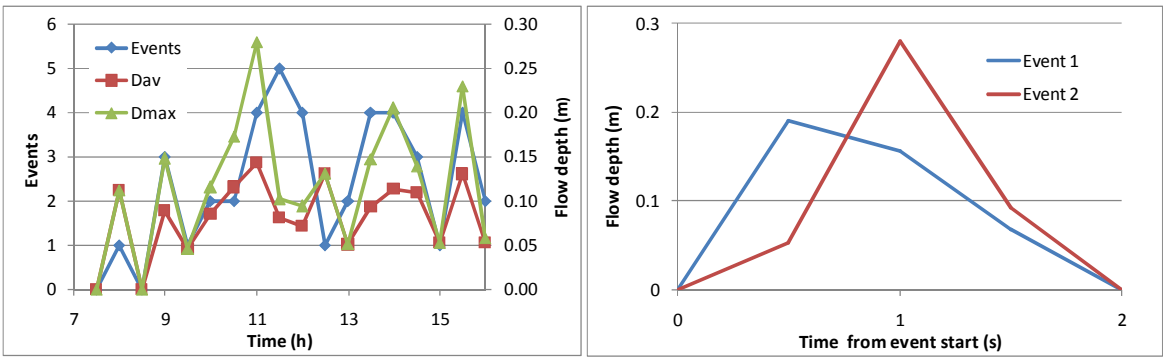

Figure 5. Number of overtopping events recorded in each half-hour block (marked at the end of the record interval), and corresponding average (Dav) and maximum (Dmax) flow depths (left panel). Two examples of distinct peaked overtoppings recorded at St3 (right panel).

The vast majority of overtopping events recorded at St3 did not reach St9, due to percolation and infiltration within the breakwater armour, or because they were just a thin water layer (smaller than 3.3 cm) not measurable by the sensor. This explains why only six events were measured at the mean crest position (St9, Figure 1), while overtopping was effectively observed and recorded at the seaward limit of the breakwater crest berm (St3, Figure 1). The six overtopping events recorded at St9 were distributed in only 3 blocks of 30 minutes (8:30-9:00 am, 10:30-11:00 am, and 3:00-3:30 pm). Flow depths at St9 were similar for all events (Dav about 0.09 m and Dmax up

to 0.12 m); the flow was laminar and flow peaks were not easy to distinguish (see red line at Figure 2). This agrees with field (and video) observations that revealed the dominance of a thin layer of laminar flow at this position.

Mean flow velocities (Uo) were computed for the six events that crossed both St3 and St9 positions (5.2 m apart) by using the time interval from the overtopping peak at those stations (Figure 2). Obtained velocities ranged from 2.08 m/s to 4.16 m/s with an average of 2.6 m/s. Overtopping front velocities were also computed by using the time interval between front overtopping arrivals at each station. These velocities were in general higher (2.08 m/s to 6.9 m/s), with an average of 3.6 m/s. Estimations of overtopping velocities were also obtained from video analysis (for a single event), using the travel time of the runup edge between established GCPs placed near the stations or between the station PT's (visible at the video and georeferenced). The obtained velocities were 4.6 m/s (using GCPs near St3 and St9) and 4.9 m/s (using St3 and St9 as GCPs). These values are comparable to the average overtopping front velocity (3.6 m/s). For discharge computation it was only used the average mean flow velocity, $\bar{U}o$ = 2.6 m/s. The obtained mean overtopping discharges ranged between $5.5*10^{-5}$ $m^3/s/m$ and $1.24*10^{-3}$ $m^3/s/m$, at St9 (Qst9) and St3 (Qst3), respectively (Table 1).

Table 1 – Number of events per 30 minutes block, measured mean overtopping discharges at St3 and St9, and corresponding computed results based on the EurOtop formulas and the NN_OVERTOPPING2 tool.

Time	Overtopping Events	St3					
		Qst3	Q_NN	Q_NN (2.5%)	Q_NN (97.5%)	Q'_NN	Q_Formula
(hour)	(#)	($m^3/s/m$)	($m^3/s/m$)	($m^3/s/m$)	($m^3/s/m$)	($m^3/s/m$)	($m^3/s/m$)
7.5	0	0.00E+00	1.29E-05	6.07E-07	2.83E-04	1.17E-04	1.00E-06
8.0	1	1.62E-04	1.86E-05	9.71E-07	3.77E-04	1.45E-04	2.00E-06
8.5	0	0.00E+00	1.61E-05	8.42E-07	2.98E-04	1.33E-04	2.00E-06
9.0	3	3.87E-04	5.03E-05	3.93E-06	8.30E-04	2.54E-04	8.00E-06
9.5	1	6.67E-05	4.39E-05	3.40E-06	6.45E-04	2.36E-04	7.00E-06
10.0	2	3.07E-04	7.81E-05	6.41E-06	1.18E-03	3.22E-04	1.50E-05
10.5	2	3.33E-04	1.18E-04	1.07E-05	1.66E-03	4.01E-04	3.60E-05
11.0	4	1.24E-03	2.70E-04	2.50E-05	3.51E-03	6.18E-04	1.13E-04
11.5	5	8.75E-04	4.11E-04	4.35E-05	5.18E-03	7.76E-04	1.74E-04
12.0	4	4.62E-04	6.54E-04	7.23E-05	7.93E-03	1.02E-03	2.81E-04
12.5	1	3.78E-04	4.55E-04	4.97E-05	4.87E-03	8.22E-04	1.96E-04
13.0	2	1.46E-04	3.93E-04	3.89E-05	4.13E-03	7.57E-04	1.52E-04
13.5	4	7.41E-04	3.83E-04	3.45E-05	4.34E-03	7.46E-04	1.15E-04
14.0	4	7.38E-04	1.68E-04	1.33E-05	2.38E-03	4.81E-04	5.00E-05
14.5	3	4.72E-04	1.45E-04	1.03E-05	2.01E-03	4.45E-04	3.40E-05
15.0	1	7.58E-05	1.16E-04	7.43E-06	1.67E-03	3.96E-04	3.00E-05
15.5	4	8.48E-04	1.18E-04	7.93E-06	1.56E-03	4.00E-04	3.60E-05

Time	Overtopping Events	St9					
		Qst9	Q_NN	Q_NN (2.5%)	Q_NN (97.5%)	Q'_NN	Q_Formula
(hour)	(#)	($m^3/s/m$)	($m^3/s/m$)	($m^3/s/m$)	($m^3/s/m$)	($m^3/s/m$)	($m^3/s/m$)
7.5	0	0.00E+00	0.00E+00	0.00E+00	0.00E+00	0.00E+00	0.00E+00
8.0	0	0.00E+00	6.55E-06	3.90E-07	1.26E-04	6.55E-05	0.00E+00
8.5	0	0.00E+00	6.35E-06	3.76E-07	1.24E-04	6.35E-05	0.00E+00
9.0	1	5.50E-05	1.54E-05	1.16E-06	2.61E-04	1.30E-04	0.00E+00
9.5	0	0.00E+00	1.52E-05	1.10E-06	2.85E-04	1.29E-04	0.00E+00
10.0	0	0.00E+00	2.52E-05	1.76E-06	4.53E-04	1.73E-04	0.00E+00
10.5	0	0.00E+00	3.19E-05	2.66E-06	5.10E-04	1.97E-04	1.00E-06
11.0	3	2.52E-04	5.61E-05	5.60E-06	8.34E-04	2.69E-04	3.00E-06
11.5	0	0.00E+00	7.61E-05	8.55E-06	1.05E-03	3.17E-04	6.00E-06
12.0	0	0.00E+00	1.08E-04	1.44E-05	1.25E-03	3.82E-04	1.30E-05
12.5	0	0.00E+00	7.41E-05	8.96E-06	8.98E-04	3.13E-04	9.00E-06
13.0	0	0.00E+00	6.32E-05	7.26E-06	6.91E-04	2.87E-04	8.00E-06
13.5	0	0.00E+00	6.13E-05	7.03E-06	7.08E-04	2.83E-04	7.00E-06
14.0	0	0.00E+00	2.89E-05	2.97E-06	3.32E-04	1.87E-04	3.00E-06
14.5	0	0.00E+00	2.56E-05	2.58E-06	3.28E-04	1.74E-04	2.00E-06
15.0	0	0.00E+00	2.00E-05	1.95E-06	2.70E-04	1.51E-04	2.00E-06
15.5	2	1.29E-04	1.95E-05	1.83E-06	2.58E-04	1.49E-04	3.00E-06

3.3 Estimated Overtopping

Mean overtopping discharges determined with the EurOtop formulas ranged between $1.0*10^{-6}$ $m^3/s/m$ and $2.8*10^{-4}$ $m^3/s/m$ at St3, and between 0 $m^3/s/m$ and $1.3*10^{-5}$ $m^3/s/m$ at St9 (Table 1). For the NN_OVERTOPPING2 tool, considering the corrected values, Q'_NN, mean overtopping discharges varied between $1.2*10^{-4}$ $m^3/s/m$ and $1.0*10^{-3}$ $m^3/s/m$ at St3 and between 0 $m^3/s/m$ and $3.8*10^{-4}$ $m^3/s/m$ at St9 (Table 1). Concerning, Q_NN (uncorrected), mean overtopping discharges varied between $1.3*10^{-5}$ $m^3/s/m$ and $6.5*10^{-4}$ $m^3/s/m$ at St3 and between 0 $m^3/s/m$ and $1.1*10^{-4}$ $m^3/s/m$ at St9 (Table 1). The obtained 95% confidence intervals for both St3 and St9 are wide, with the upper limit being about two orders of magnitude higher than the lower one, which gives an idea of the reliability of the predictions obtained for these small overtopping conditions. Moreover, for almost 90% of the cases at St9 and for 30% of the St3 cases, the NN_OVERTOPPING2 tool gave warning messages relating that the non-dimensional computed discharges were very small (10^{-6} $m^3/s/m$ < $Q\_NN/(gHst^3)^{0.5}$ < 10^{-5} $m^3/s/m$), meaning that the NN_OVERTOPPING2 estimates were less reliable and should only be taken as indicative.

4. Discussion

4.1 Measured Overtopping *versus* Pn

Overtopping occurrence (number of events) and flow depths did not show a direct relation with both tidal level and wave heights. The higher number of events and flow depths are not centred on the high tide, and neither solely related with higher Hso values. Events occurrence is irregular along the studied tidal cycle with the majority of the overtopping events occurring after high tide. Pn is a better descriptor of the overtopping occurrence distribution and of its deviation towards ebb (Figure 6). Pn incorporates the wave height increase during ebb that balanced the tidal level decrease, explaining the continuity of overtopping occurrence at the structure. Although there is a trend for depth flow increase with an increase on Pn values (Figure 6) the relationship is not statistically significant and Pn cannot be used as a single proxy to describe the discharges variability for small overtopping conditions. From the results it can be concluded that overtopping was not recorded (or had a small expression) at St3 (seaward crest berm) for Pn < 40000 J/m/s.

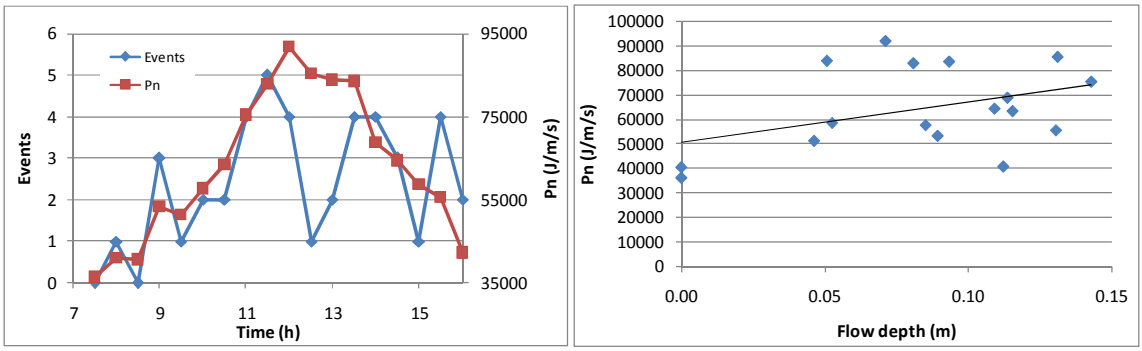

Figure 6. Pn behaviour compared to the number of events recorded at St3 along the studied period (left panel) and the observed relationship between Pn and measured flow depth (right panel).

4.2 Measured *versus* Estimated Overtopping

NN_OVERTOPPING2 estimated discharges presented relatively small variations along the studied period, while the measured discharges at St3 revealed higher variability, mainly during ebb (Figure 7). Average discharges provided by NN_OVERTOPPING2 (corrected) are reasonably similar to the measured mean discharges, when considering the entire period of analysis. However, differences can be substantial when comparing each block individually. At St3 the mean relative

error between Qst3 and Q'_NN is about 77%, whereas the maximum relative error is of 422% (for t=15 h). At St9, where only six overtopping events occurred during three half-hour blocks, the mean relative error between Qst9 and Q'_NN is smaller, about 53%, whereas the maximum relative error is of 153% (for t=9 h). The measured discharges at both locations fall always within the 95% confidence intervals of the NN_OVERTOPPING2 tool. The correction applied by this tool improves significantly the agreement between measured and predicted discharges (Figure 7).

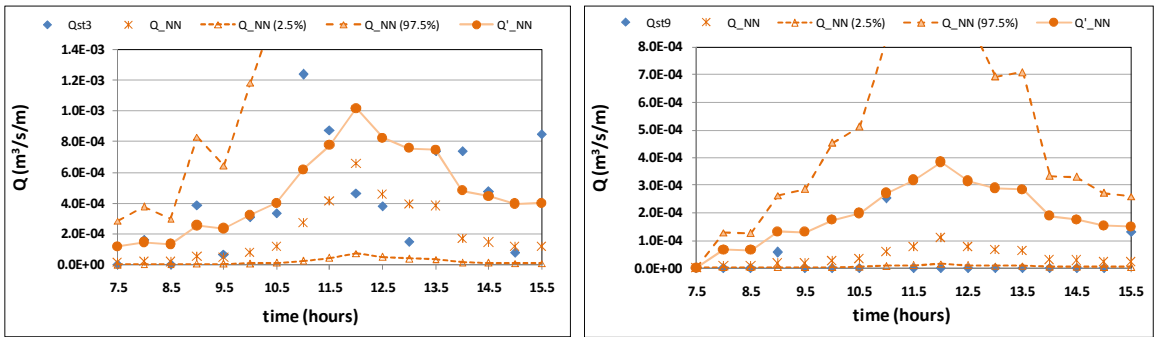

Figure 7. Measured mean overtopping discharges at St3 (left panel) and St9 (right panel) compared to the estimated discharges from the NN_OVERTOPPING2 tool: corrected (Q'_NN), uncorrected (Q_NN) and the 95% confidence intervals ([Q_NN(2.5%); Q_NN(97.5%)]).

There is a good agreement between Q'_NN and Qst3, with most of the data points lying in the range of 1/2<Q'_NN/Qst3<2 (Figure 8). The tool tends, however, to overestimate the smaller discharges. At St9, the measured mean overtopping discharges are well predicted by the NN_OVERTOPPING2 tool (Figure 8). In contrast, the EurOtop formulas clearly underestimate the discharges at both St3 and St9 by one or even two orders of magnitude (Figure 8, Table 1). A similar situation occurs for the uncorrected NN_OVERTOPPING2 results (Table 1).

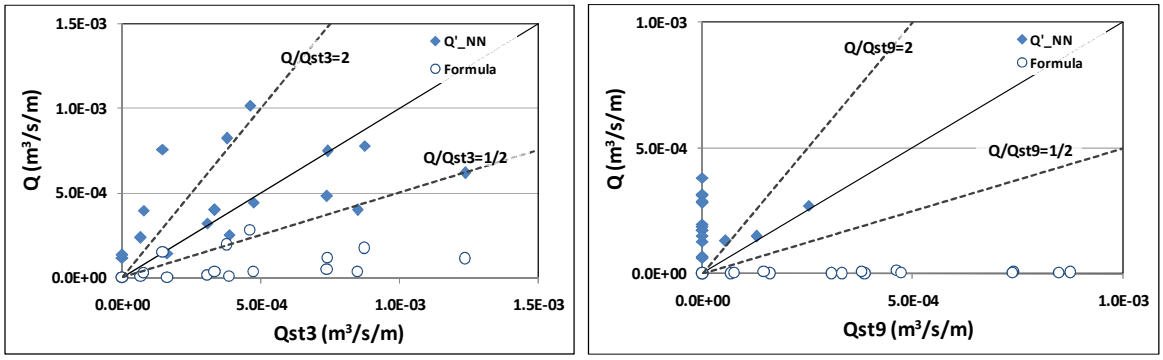

Figure 8. Measured mean overtopping discharges at St3 (left panel) and St9 (right panel) and the estimated discharges from the EurOtop formulas (Formula) and the NN_OVERTOPPING2 tool (Q'_NN)

NN_OVERTOPPING2 can be used to characterise the overall discharge for the analysed conditions – small overtopping near the occurrence limit - but it will have important errors when assessing detailed short period events. That can be explained by the gradual changes on both wave and tidal behaviour along the studied period that contrast with the irregularity on overtopping from block to block, meaning that non-linear factors (such as wave-wave interaction, wave groupiness or nearshore wave transformation) may have a great influence on the overtopping process. Deviations between fieldwork data and tool estimates can also be justified by difficulties inherent to the overtopping measurement at the field. For instance, it was not possible to measure flow depths smaller than 4.6 cm (St3) and 3.3 cm (St9), even if they have been confirmed by *in situ* observations (visual or using video imagery). Thus, for several half-hour blocks, small overtopping

events may have happened but were not recorded. This is particularly important in thin near bed laminar flows, such as the ones at St9. EurOtop formulations and uncorrected NN_OVERTOPPING2 do not seem suitable to reliably predict small overtopping discharges for the analysed conditions and, therefore, their results should be taken as indicative only.

4.3 Pn *versus* NN_OVERTOPPING2

Pn (Figure 4, right panel) presents an analogous behaviour to the discharges estimated by the corrected NN_OVERTOPPING2 for St3 (Figure 7), with a high correlation level between values (R^2 = 0.964, p<0.01; Figure 9). Therefore, Pn can be cautiously used as a simple proxy to estimate discharges at the seaward berm crest, with a level of confidence similar to NN_OVERTOPPING2. For the studied conditions the obtained relationship is:

$$Q'\_NN = 1.55 \times 10^{-8}\text{Pn} - 5.22 \times 10^{-4} \quad (4)$$

where Q'_NN is the estimated discharge using corrected NN_OVERTOPPING2 (or a discharge to be predicted by Pn). This simple equation can be used to predict discharges along a tidal cycle, at the seaward berm crest (St3 position), without being able to represent discharge peaks or strong variations along that cycle. An advantage is the use of estimated sea levels and offshore wave heights (without needing propagation) to predict discharges for some time in advance (days) at the structure. It is however expected that the relationship between Pn and estimated discharge varies from structure to structure since discharges depend on the structure characteristics.

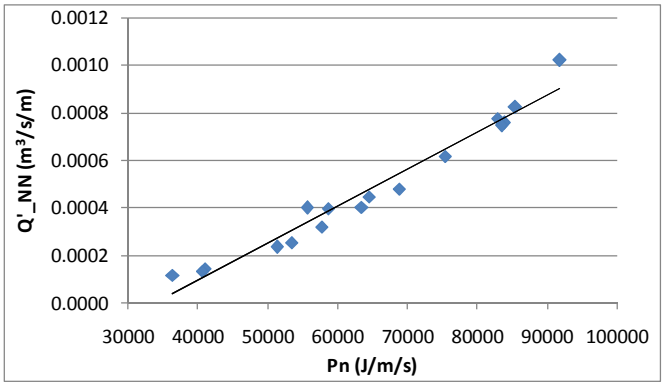

Figure 9. Linear relationship between Pn and Q'_NN for St3.

5. Conclusions

This study presents the first data set of wave overtopping measured at a breakwater in Portugal, including flow depths, velocities and discharges. The study compares overtopping discharges measured at the breakwater with discharges estimated by empirical methods, for small overtopping conditions. Measurements were performed at limiting hydrodynamic conditions, which poses difficulties on measuring the flow and also represents a challenge for the existing models and empirical methods. The corrected NN_OVERTOPPING2 was the methodology that better represented the measured discharges. Nevertheless, the method had difficulties to replicate the observed short-term variability along the monitored period. The EurOtop formulas and the uncorrected NN_OVERTOPPING2 were unable to properly predict the discharges and seem not suitable to reliably estimate small overtopping conditions. As a consequence, results from their application at such conditions should be regarded as indicative only. The normalized wave power (Pn), integrating offshore waves and sea level conditions, is proposed as a proxy for fast, easy and in advance overtopping estimation with results comparable to the corrected NN_OVERTOPPING2 predictions, for the study case. This proxy needs to be further tested and validated at other structures and hydrodynamic conditions.

Acknowledgements

This work is a contribution to the project SPACE (PTDC/ECM/114109/2009), funded by Fundação para a Ciência e a Tecnologia, Portugal. The authors are grateful to André Pacheco for helping during field work, to Ana Matias for the discussions on the overtopping flow definition, and to Alex Garcia for performing video analysis. Tidal data were kindly supplied by Puertos del Estado and offshore wave data by Instituto Hidrográfico.

References

Coeveld, E.M., Van Gent, M.R.A., Pozueta, B. (2005). *Neural Network. Manual NN_OVERTOPPING 2. CLASH WP8*, WL Delft Hydraulics Report, Delft, The Netherlands.

De Rouck, J., Geeraerts, J., Troch, P., Kortenhaus, A., Pullen, T., Franco, L. (2005). New results on scale effects for wave overtopping at coastal structures. *Proc. ICE Coastlines, Structures & Breakwaters '05*, Thomas Telford, London, pp. 29-43.

McCabe, M. V., Stansby, P. K., Apsley, D. D., (2013). Random wave runup and overtopping a steep sea wall: Shallow-water and Boussinesq modelling with generalised breaking and wall impact algorithms validated against laboratory and field measurements. *Coastal Engineering*, 74, 33-49.

Morris, B.D., Davidson, M.A., Huntley, D.A. (2001). Measurements of the response of a coastal inlet using video monitoring techniques. *Marine Geology*, 175, 251-272.

Norgaard, J.Q.H., Andersen, T.L., Burcharth, H.F., Steendam, G.J. (2013). Analysis of overtopping flow on sea dikes in oblique and short-crested waves. *Coastal Engineering*, 76, 43-54.

Pullen, T., Allsop, N.W.H., Bruce, T., Kortenhaus, A., Schuttrumpf, H.,Van der Meer, J.W. (2007). *EurOtop: Wave Overtopping of Sea Defences and Related Structures: Assessment Manual*. Environment Agency, UK, Expertise Netwerk Waterkeren, NL, and Kuratorium fur Forschung im Kusteningenieurwesen, DE.

Internet references:

Crest Level Assessment of Coastal Structures by full scale monitoring, neural network prediction and Hazard Analysis on permissible wave overtopping, 2001. EU-project CLASH. www.clash.ugent.be. (assessed April 2013)

EurOtop - Wave overtopping of sea defences and related structures: Assessment manual, 2008. Calculation Tool, HR Wallingford Ltd. http://www.overtopping-manual.com/calculation_tool.html (assessed April 2013)

Java Applets for Coastal Engineering, 2003. University of Delaware Wave Calculator. http://www.coastal.udel.edu/faculty/rad/ (assessed April 2013)